Reconnection and Turbulence in Space Plasmas on Kinetic Scales

Wiesław M. Macek[1,2]

[1] Faculty of Mathematics and Natural Sciences
Cardinal Stefan Wyszyński University
Wóycickiego 1/3, 01-938 Warsaw, Poland
[2] Space Research Centre, Polish Academy of Sciences
Bartycka 18 A, 00-716 Warsaw, Poland
(E-mail: macek@cbk.waw.pl)

Abstract. Turbulent magnetic fields play an important role in plasmas leading to magnetic reconnection, which is a complex phenomenon that still remains a challenge for contemporary physics. We have already considered magnetic turbulence using observations from the *Magnetospheric Multiscale* (*MMS*) mission on kinetic (ions and electron) scales, which are far shorter than the scales characteristic for description of plasma by magnetohydrodynamic (MHD) theory. In particular, we have shown that a clear break of the magnetic spectral exponent to about -11/2 at frequencies 20 – 25 Hz agrees with the predictions of kinetic theory (-16/3) Ref. [10]. It is worth noting that the unprecedented very high (millisecond) resolution of the magnetic field instrument enabled us to grasp the mechanism of reconnection in the magnetotail on ion and electron scale lengths [11]. As expected from numerical simulations, we have verified that when the field lines and plasma become decoupled a large reconnecting electric field related to the Hall current (1–10 mV/m) is responsible for fast reconnection in the ion diffusion region both at the magnetopause and in the magnetotail regions. Although inertial accelerating forces remain moderate (1–2 mV/m), the electric fields resulting from the divergence of the full electron pressure tensor provide the main contribution to the generalized Ohm's law at the neutral sheet (of the order of 100 mV/m), see Ref. [12]. In our view, this illustrates that when ions decouple electron physics dominates. The results obtained on kinetic scales may be useful for better understanding the physical mechanisms governing reconnection processes in various magnetized plasmas in the Universe.
Keywords: Reconnection, Turbulence, Space plasmas, Magnetohydrodynamics, Kinetic theory.

1 Introduction: Importance of Reconnection

Turbulent magnetic fields play an important role in space environments [2], leading to magnetic reconnection in space plasmas [1,4,6,18,19,22–24]. Notwithstanding great progress in theoretical studies employing computer simulations within magnetohydrodynamic (MHD; Hall-MHD, two-fluid) theory, the physical mechanism for reconnection still remains a challenge for contemporary

13th CHAOS Conference Proceedings, 9 - 12 June 2020, Florence, Italy

© 2020 ISAST

science. Admittedly, the reconnection processes on the Sun or in remote astrophysical systems in the Universe cannot be studied directly *in situ*. However, the solar wind is a stream of charged particles (mainly ions and electrons) flowing from the Sun with the embedded interplanetary magnetic field (IMF). Interaction of this plasma of solar origin that fills-up the Solar System with the Earth dipole magnetic field results in the terrestrial magnetosphere including the magnetopause, plasmasheet, and magnetotail displayed in Fig. 1. The structure of the Earth's magnetosphere is controlled by reconnection. Hence, the terrestrial magnetosphere could be considered a natural laboratory for investigating the reconnection processes responsible for the redistribution of kinetic and magnetic energy in space environments and laboratory plasmas. As is known, reconnection occurs in two main regions of the magnetosphere: the dayside magnetopause and the nightside magnetotail, which are marked by red boxes in Fig. 1.

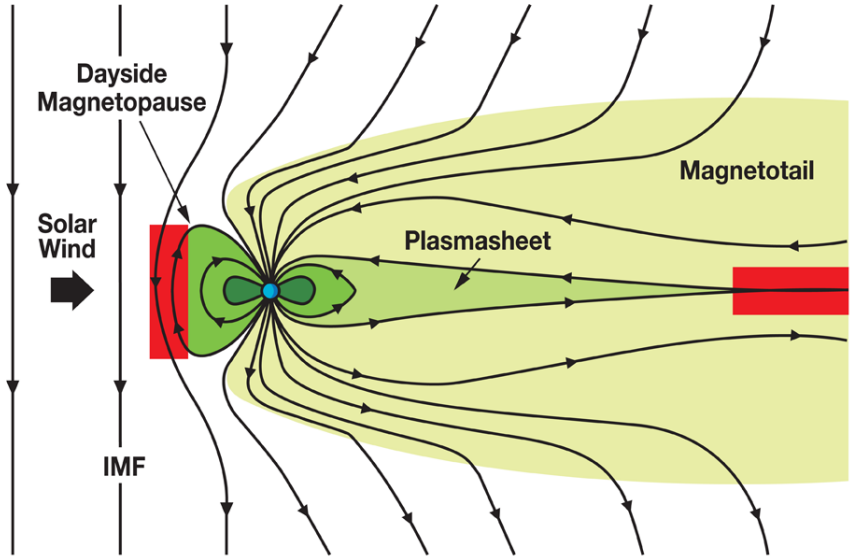

Fig. 1. Reconnection in the magnetosphere

One of the the main objectives of the *Magnetospheric Multiscale* (*MMS*) mission is to determine the role of turbulence in the reconnection processes and the roles of ions and electrons in these processes. Reconnection occurs mainly when the electrons cannot supply the current needed to support antiparallel magnetic fields. Inflowing plasma curries oppositely directed magnetic field lines into the ion (IDR, in blue) and electron (EDR, in pink) diffusion regions, as sketched in Fig. 2. The four *MMS* spacecraft (marked by red crosses) make the measurements needed to determine the processes that drive reconnection.

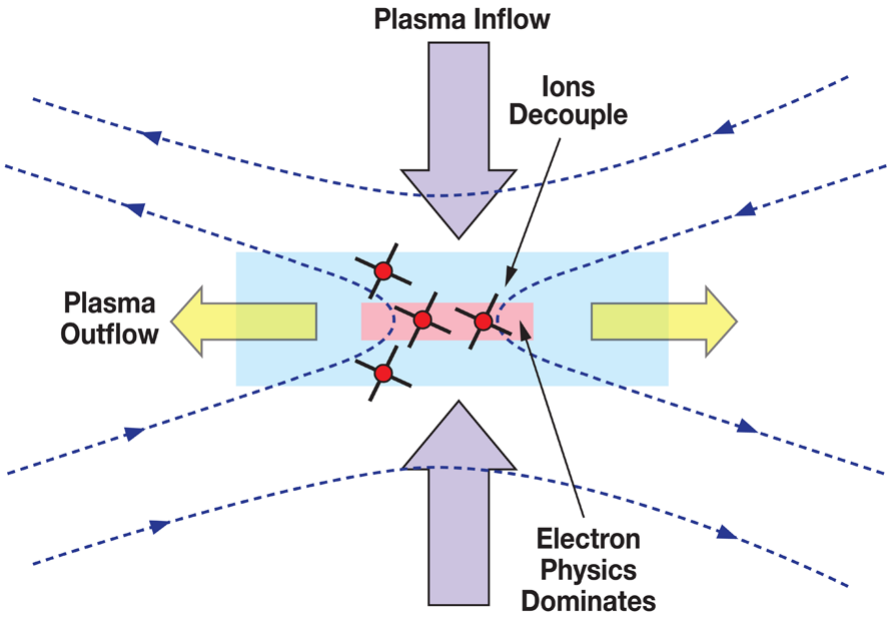

Fig. 2. Mechanism of reconnection

1.1 Research Hypothesis

- Reconnection depends on the deviations from MHD, including Hall-MHD, electron pressure, and inertia effects on both ion and electron scales as seen in the *MMS* data.
- Hence, our basic research hypothesis is that the gross features of reconnection should be determined by small scales, which are essential for understanding of the physical mechanisms of reconnection. In our view, it is necessary to investigate the experimental data at scale lengths below the magnetohydrodynamic scales.
- This naturally leads to a description of space plasmas within kinetic theory, instead of an ideal MHD approach.

Following our previous study of turbulence and reconnection using *MMS* data [10–12], we analyze the electric fields on sub-ion scales at the magnetopause and in the magnetotail near the X-line within highly variable plasmas to compare the characteristics of reconnection processes in both regions shown in Fig. 1, when going from the ion to electron kinetic scales, Fig. 2.

2 Data from the MMS Mission

The *MMS* mission was launched on 13 March 2015 at 02:44 UTC, as illustrated in Fig. 3. The planned mission duration was 2 years, 5.5 months, but now is

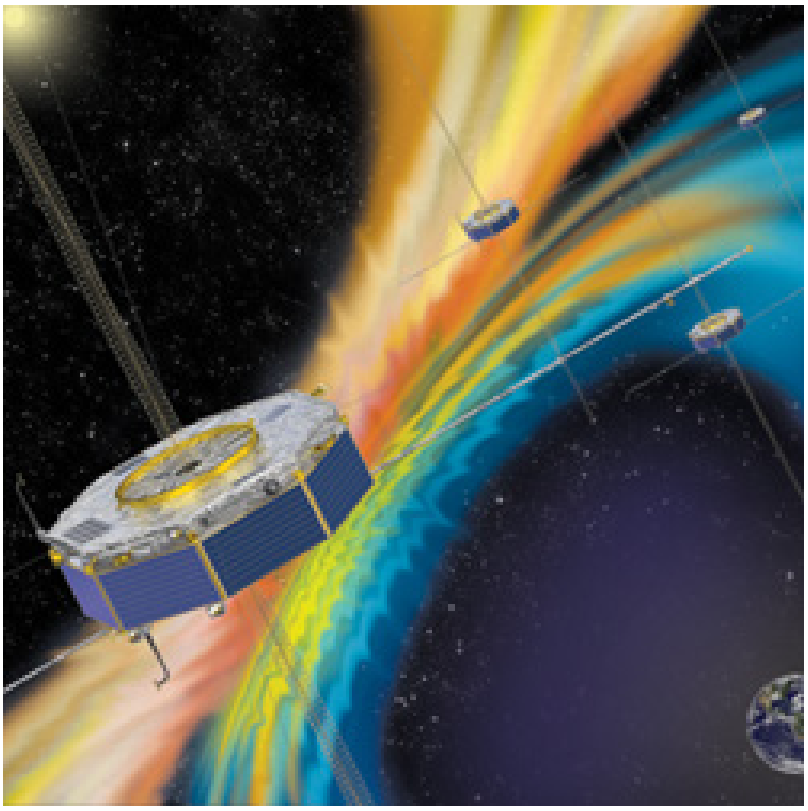

Fig. 3. The *MMS* is a NASA unmanned space mission to study the Earth's magnetosphere, using the four identical spacecraft flying in a tetrahedral formation, Credits: NASA.

in its $5th$ year of operation, and its characteristics are, as follows, launch mass: 1,360 kg (2,998 lb); inclination: 28.0°; perigee: 2,550 km (1,580 mi); apogee: day phase: 70,080 km (43,550 mi); night phase: 152,900 km (95,000 mi). The location and formation of four spacecraft near the apogee are depicted in Fig. 4 and 5, respectively.

MMS is also equipped with a new navigator based on extremely sensitive GPS equipment to provide absolute position information, Figs. 6 and 7. The observatories require such sensitive sensors because the satellites fly in an orbit higher than that of the GPS satellites, so they must rely on the weaker signals from GPS satellites on the far side of the Earth. The *MMS* spacecraft were developed at NASA's Goddard Space Flight Center in Greenbelt, MD, USA.

In situ evidence for the reconnection diffusion regions (IDR, EDR) at the dayside magnetopause using *MMS* measurements in a case study on 16 October 2016 was discussed in Ref. [3,20]. A list of 32 such magnetopause events has also been reported in Ref. [26]. Observations of electron scale structures and magnetic reconnection signatures in the turbulent magnetosheath using *MMS* measurements are also reported [27], including reconnection jets at the

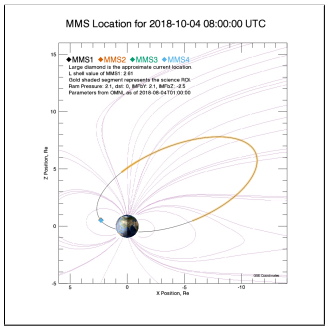

Fig. 4. MMS Location

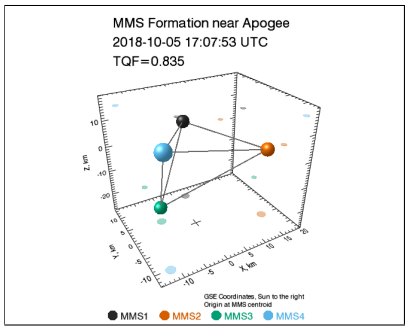

Fig. 5. MMS formation

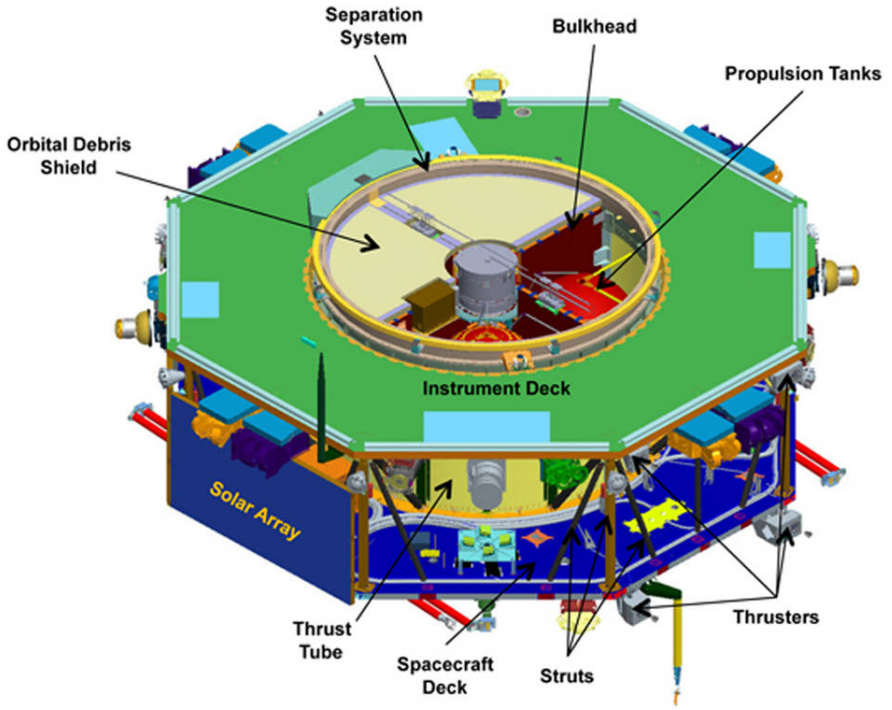

Fig. 6. Illustration of MMS spacecraft with systems labeled, Credits: NASA.

magnetopause [14] and a current plasmasheet on electron scales in the near-Earth magnetotail without bursty reconnection [25]. By contrast, a reconnection event on 11 July 2017 in also studied in Ref. [21]. The authors reported that the spacecraft entered the EDR in the magnetotail, suggesting that electron dynamics in this region was mostly laminar despite turbulence near the reconnection region. A kinetic simulation of magnetopause reconnection are provided in Ref. [5], while simulation results for a magnetotail case are given in Ref. [13]. *MMS* observations of an electron-scale magnetic cavity embedded in

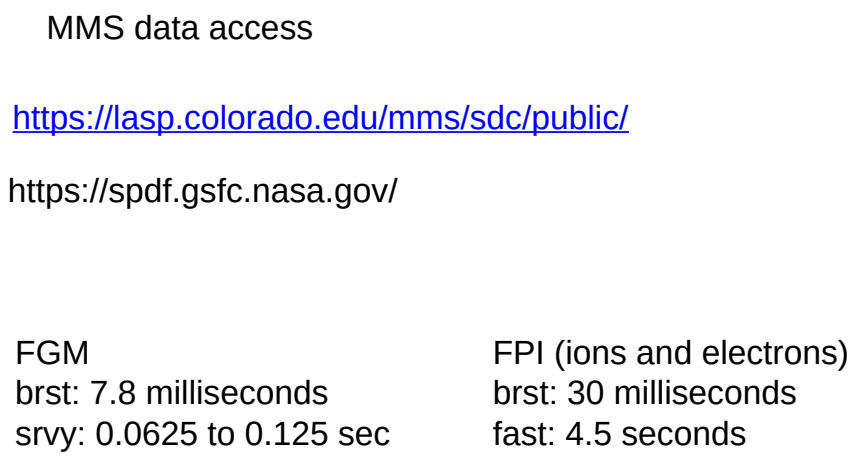

Fig. 7. MMS data access and resolution

a proton-scale cavity are also found [9]. One can hence expect that a detailed analysis of the high-resolution *MMS* data will provide significant insight into the nature of reconnection processes in space plasmas.

3 Methods of Data Analysis

In the one-fluid magnetohydrodynamic (MHD) theory the electric field, $\mathbf{E}'_{\rm o} = \mathbf{E} + \mathbf{V} \times \mathbf{B}$, is seen in the rest frame for the plasma moving with the velocity $\mathbf{V}$, see Ref. [8]. In a case of the ideal fluid (with zero resistivity) this should be equal to zero, but in the case of a more realistic two-fluid theory, consisting of ion and electron components (denoted herein by subscript i and e, respectively), the Hall term $\mathbf{E}_{\rm H} = -\mathbf{j} \times \mathbf{B}/(en)$, with the electron elementary charge e, density $n = n_{\rm i} = n_{\rm e}$, and the current density $\mathbf{j} = {\rm e}(n_{\rm i}\mathbf{V}_{\rm i} - n_{\rm e}\mathbf{V}_{\rm e})$, should be taken into account: $\mathbf{E}' \equiv \mathbf{E}'_{\rm o} + \mathbf{E}_{\rm H}$. In the reconnection region the difference of the acceleration of electrons and ions ${\rm e}\mathbf{E}_{\rm a} = m_{\rm e}{\rm d}(\mathbf{V}_{\rm e} - \mathbf{V}_{\rm i})/{\rm d}t$ should result in an additional inertial term, $\mathbf{E}_{\rm a}$.

It is important noting that according to our research hypothesis (subsection 1.1), on very small kinetic scales when electrons decouple from ions, as schematically sketched in Fig. 2., the nonideal contribution to the electric field should result from the divergence of the fully anisotropic pressure (dyadic) tensor [7],

$$\mathbf{P} \equiv m \int (\mathbf{V} - \mathbf{U})(\mathbf{V} - \mathbf{U}) f {\rm d}^3\mathbf{V}. \tag{1}$$

Note that by averaging over velocity space for a given position $\mathbf{r} = (x, y, z)$ within an infinitesimally small fluid element of volume ${\rm d}^3\mathbf{r} = {\rm d}x{\rm d}y{\rm d}z$, one can write $\mathbf{P} = mn < (\mathbf{V} - \mathbf{U})(\mathbf{V} - \mathbf{U}) >$ [17]. This means that the pressure term should have a somewhat similar structure to that of the inertial term, but with the distribution function f for individual particles moving randomly

with velocities $\mathbf{V}$ around the mean (bulk) velocity $\mathbf{U} \equiv < \mathbf{V} >= \frac{1}{n}\int \mathbf{V} f \mathrm{d}^3\mathbf{V}$. Because $m_\mathrm{e}/m_\mathrm{i} \ll 1$, the contribution from the ion pressure tensor can be neglected and we only have the electron tensor electric field [16]:

$$\mathbf{E}_\mathrm{p} \equiv \frac{1}{en_\mathrm{e}}\nabla \cdot \mathbf{P}_\mathrm{e} = \frac{m_\mathrm{e}}{en_\mathrm{e}}\nabla \cdot [n_\mathrm{e} < (\mathbf{V}_\mathrm{e} - \mathbf{U})(\mathbf{V}_\mathrm{e} - \mathbf{U}) >], \tag{2}$$

where the diagonal thermal pressures are given by $p_{\|\mathrm{e}} = n_\mathrm{e} k_\mathrm{B} T_{\|\mathrm{e}}$ and $p_{\perp\mathrm{e}} = n_\mathrm{e} k_\mathrm{B} T_{\perp\mathrm{e}}$, parallel and perpendicular with regard to the magnetic field $\mathbf{B}$, and k_B is the Boltzmann constant, $T_{\|\mathrm{e}} + 2T_{\perp\mathrm{e}} = Tr\mathbf{T}_\mathrm{e}$, including the off-diagonal components are responsible for non-gyrotropic (crescent) features of the electron distribution function f_e and the temperature tensor $\mathbf{T}_\mathrm{e} \equiv \mathbf{P}_\mathrm{e}/(nk_\mathrm{B})$.

FPI L2 DES/DIS Moments -- Methodology

FPI plasma moments are calculated as follows:

Quantity	
Number Density:	n = int(f d^3v)
Bulk Velocity Vector:	**U** = int(f **v** d^3v) / n
Pressure Tensor:	$\underline{\mathbf{P}}$ = m*int(f (v-**U**) (v-**U**) d^3v)
Temperature Tensor:	$\underline{\mathbf{T}}$ = $\underline{\mathbf{P}}$ / (n k_B)
Parallel Temperature:	$T_{\|\|}$ = (**b**^{T} $\underline{\mathbf{T}}$ **b**)
Perpendicular Temperature:	T_{perp} = (Tr($\underline{\mathbf{T}}$) – $T_{\|\|}$) / 2
Heat Flux Vector:	**q** = m * int(f **v** v^2 d^3v) / 2 – (nmU^2)*$\mathbf{U}$ / 2 – ((Tr $\underline{\mathbf{P}}$/2) $\underline{\mathbf{I}}$ + $\underline{\mathbf{P}}$)□ • $\underline{\mathbf{U}}$

where **b** is the unit vector of the magnetic field averaged over the measurement interval

Fig. 8. MMS data moments

All theses moments of plasma parameters (density n, velocity U, pressure tensor $\mathbf{P}$, temperatures $T_\|$ and $T_\perp$ can be calculated by using the Dual Ions and Electron Spectrometer (DIS, DES) instruments of Ref. [15], shown in Fig. 6, as summarized in Fig. 8.

Finally, the sum of all the contributions to the electric field, $\mathbf{E}_\mathrm{tot}$, consisting of various terms

$$\mathbf{E}_\mathrm{tot} = \mathbf{E}'_\mathrm{o} + \mathbf{E}_\mathrm{H} + \mathbf{E}_\mathrm{a} + \mathbf{E}_\mathrm{p}, \tag{3}$$

where $\mathbf{E}'_\mathrm{o}$, $\mathbf{E}_\mathrm{H}$, $\mathbf{E}_\mathrm{a}$, and $\mathbf{E}_\mathrm{p}$ denote the ideal, and the respective nonideal Hall, inertial, and pressure contributions should be equal to the dissipation $\eta\mathbf{j}$ created by an anomalous resistivity η, which is called the generalized Ohm's law [16].

The electric field given by Equation (2) becomes important in the region where ions decouple and electron physics dominate, Fig. 2. Hence, we propose that the ratio of the thermal pressure term $\mathbf{E}_\mathrm{p}$ of Equation (2) to the sum of other terms including the ideal $\mathbf{E}'_\mathrm{o}$ with Hall term $\mathbf{E}_\mathrm{H}$, and the electron (inertial) accelerating $\mathbf{E}_\mathrm{a}$ contributions,

$$r_\mathrm{e} \equiv |\mathbf{E}_\mathrm{p}|/|\mathbf{E}'_\mathrm{o} + \mathbf{E}_\mathrm{H} + \mathbf{E}_\mathrm{a}|, \tag{4}$$

to be a useful signature indicating approaches to the EDR.

4 Observations of Reconnection Electric Fields

We have thoroughly discussed the plasma and magnetic field data together with various components of the electric fields responsible for reconnection in the magnetotail. Namely, following various observations of reconnection in the dayside magnetopause [26] and one case in the nightside magnetotail [21], as displayed (in red) in Fig. 1, we have studied three new *MMS* events at the current sheet crossings on 23 and 24 July 2018, see Ref. [11]. The observed magnetic field reversal on current sheet approach is followed by an ion flow reversal, but with large fluctuations in the electron velocity. Compared with the temperature asymmetry observed in the EDR of July 2017, this approach to the neutral sheet charged particle exhibit some heating, up to energies of a few tens keV for ions and 1–10 keV for electrons, but with rather isotropic ion (3–6 keV) and electron temperatures (2–3 keV).

These newly observed electric fields when approaching the EDR [11], cases (c–e), together with the first crossing of the EDR in the magnetotail by *MMS* on 11 July 2017 reported in Ref. [21] on the night side magnetosphere, case (b), were then compared with those at the magnetopause, Ref. [12], case (a). The estimated values for all these selected cases (a–e) are now displayed in Table 1.

Table 1. List of selected *MMS* spacecraft (s-c) interval samples in the magnetopause (a) and the magnetotail (b – e) (hh.min:ss) with the current $\mathbf{j}(\mu\mathrm{A/m2})$, the ideal $\mathbf{E}'_\mathrm{o}$ (mV/m) and the nonideal Hall, inertial, and pressure contributions, $\mathbf{E}_\mathrm{H}$, $\mathbf{E}_\mathrm{a}$, and $\mathbf{E}_\mathrm{p}$, respectively, together with the parameter r_e indicating approaches to the electron diffusion region (EDR)

Case	S-c	Time (y.m.d)	Begin	End	$\mathbf{j}$	$\mathbf{E}'_\mathrm{o}$	$\mathbf{E}_\mathrm{H}$	$\mathbf{E}_\mathrm{a}$	$\mathbf{E}_\mathrm{p}$	r_e
(a)	2	2016.11.23	07.49:32	07.49:35	0.45	5–10	8	0.1–0.3	1–2.5	0.10
(b)	3	2017.07.11	22.34:01	22.34:05	0.064	3–8	12	1–2.5	2–3	0.08
(c)	2	2018.07.23	11.37:57	11.38:05	0.009	1–5	0.7	0.1–0.3	8–10	1.5
(d)	1–3	2018.07.24	17.46:33	17.46:41	0.037	1–1.5	0.25	0.15–0.25	100–200	90
(e)	1–3	2018.07.24	17.47:06	17.47:14	0.0056	$\lesssim$0.8	0.2	1–3	100–200	200

5 Conclusions

In addition to ideal electric fields, our cases exhibit large electric field comparable in magnitude (1–10 mV/m) to those associated with the Hall current, which together with the rather moderate inertial accelerating fields (1–2 mV/m), are responsible for fast reconnection in the ion diffusion region (IDR). However, during the approaches to the electron diffusion region (EDR), as indicated by a large value of our newly devised reconnection parameter r_e of Equation (4), the electric fields $\mathbf{E}_p$ arising from the divergence of the full electron pressure tensor $\mathbf{P}_e$ according to Equation (2) provide the main contribution (as large as 100–200 mV/m) to the generalized Ohm's law, see Equation (3); both regions are marked in Fig. 2. We can hence expect that when ions decouple electron kinetic physics should provide the mechanisms responsible for reconnection processes. The *MMS* mission may also be useful for better understanding the physical mechanism governing reconnection processes in various laboratory and astrophysical plasmas.

Acknowledgments. We are grateful for the dedicated efforts of the entire *MMS* mission team, including development, science operations, and the Science Data Center at the University of Colorado. We especially benefited from the efforts of C. J. Pollock, and C. T. Russell and the magnetometer team for providing the magnetic field data, available online from http://cdaweb.gsfc.nasa.gov. We acknowledge T. E. Moore, Project Scientist, and M. L. Adrian, Deputy Project Scientist, for discussions on the field and plasma instruments. This work has been supported by the *MMS* project through the Catholic University of America during a visit by W. M. Macek to the NASA Goddard Space Flight Center.

References

1. D. Biskamp. *Magnetic Reconnection in Plasmas*, volume 3 of *Cambridge monographs on plasma physics*. Cambridge, UK: Cambridge University Press, 2000.
2. R. Bruno and V. Carbone. *Turbulence in the Solar Wind*, volume 928 of *Lecture Notes in Physics*. Springer International Publishing, Berlin, 2016.
3. J. L. Burch, R. B. Torbert, T. D. Phan, L.-J. Chen, T. E. Moore, R. E. Ergun, J. P. Eastwood, D. J. Gershman, P. A. Cassak, M. R. Argall, S. Wang, M. Hesse, C. J. Pollock, B. L. Giles, R. Nakamura, B. H. Mauk, S. A. Fuselier, C. T. Russell, R. J. Strangeway, J. F. Drake, M. A. Shay, Y. V. Khotyaintsev, P.-A. Lindqvist, G. Marklund, F. D. Wilder, D. T. Young, K. Torkar, J. Goldstein, J. C. Dorelli, L. A. Avanov, M. Oka, D. N. Baker, A. N. Jaynes, K. A. Goodrich, I. J. Cohen, D. L. Turner, J. F. Fennell, J. B. Blake, J. Clemmons, M. Goldman, D. Newman, S. M. Petrinec, K. J. Trattner, B. Lavraud, P. H. Reiff, W. Baumjohann, W. Magnes, M. Steller, W. Lewis, Y. Saito, V. Coffey, and M. Chandler. Electron-scale measurements of magnetic reconnection in space. *Science*, 352:aaf2939, June 2016.
4. L. F. Burlaga. *Interplanetary Magnetohydrodynamics*. New York: Oxford University Press, 1995.

5. W. Daughton, T. K. M. Nakamura, H. Karimabadi, V. Roytershteyn, and B. Loring. Computing the reconnection rate in turbulent kinetic layers by using electron mixing to identify topology. *Phys. Plasmas*, 21(5):052307, May 2014.
6. P. Figura and W. M. Macek. Model of line preserving field line motions using Euler potentials. *Annals of Physics*, 333:127–135, 2013.
7. D. A. Gurnett and A. Bhattacharjee. *Introduction to Plasma Physics*. Cambridge, UK: Cambridge University Press, January 2005.
8. N. A. Krall and A. W. Trivelpiece. *Principles of Plasma Physics*. International Series in Pure and Applied Physics. New York: McGraw-Hill Book Co., 1973.
9. H. Liu, Q. G. Zong, H. Zhang, C. J. Xiao, Q. Q. Shi, S. T. Yao, J. S. He, X. Z. Zhou, C. Pollock, w. J. Sun, G. Le, J. L. Burch, and R. Runking. M m s observations of electron scale magnetic cavity embedded in proton scale magnetic cavity. *Nat. Commun.*, 10(1):1040, 2019.
10. W. M. Macek, A. Krasińska, M. V. D. Silveira, D. G. Sibeck, A. Wawrzaszek, J. L. Burch, and C. T. Russell. Magnetospheric multiscale observations of turbulence in the magnetosheath on kinetic scales. *Astrophys. J. Lett.*, 864(2):L29, 2018.
11. W. M. Macek, M. V. D. Silveira, D. G. Sibeck, B. L. Giles, and J. L. Burch. Magnetospheric Multiscale Mission Observations of Reconnecting Electric Fields in the Magnetotail on Kinetic Scales. *Geophys. Res. Lett.*, 46(10295):10,295–10,302, Sep 2019.
12. W. M. Macek, M. V. D. Silveira, D. G. Sibeck, B. L. Giles, and J. L. Burch. Mechanism of Reconnection on Kinetic Scales Based on Magnetospheric Multiscale Mission Observations. *Astrophys. J. Lett.*, 885(1):L26, Nov 2019.
13. T. K. M. Nakamura, K. J. Genestreti, Y.-H. Liu, R. Nakamura, W.-L. Teh, H. Hasegawa, W. Daughton, M. Hesse, R. B. Torbert, J. L. Burch, and B. L. Giles. Measurement of the Magnetic Reconnection Rate in the Earth's Magnetotail. *J. Geophys. Res.*, 123:9150–9168, November 2018.
14. M. Øieroset, T. D. Phan, C. Haggerty, M. A. Shay, J. P. Eastwood, D. J. Gershman, J. F. Drake, M. Fujimoto, R. E. Ergun, F. S. Mozer, M. Oka, R. B. Torbert, J. L. Burch, S. Wang, L. J. Chen, M. Swisdak, C. Pollock, J. C. Dorelli, S. A. Fuselier, B. Lavraud, B. L. Giles, T. E. Moore, Y. Saito, L. A. Avanov, W. Paterson, R. J. Strangeway, C. T. Russell, Y. Khotyaintsev, P. A. Lindqvist, and K. Malakit. MMS observations of large guide field symmetric reconnection between colliding reconnection jets at the center of a magnetic flux rope at the magnetopause. *Geophys. Res. Lett.*, 43:5536–5544, June 2016.
15. C. Pollock, T. Moore, A. Jacques, J. Burch, U. Gliese, Y. Saito, T. Omoto, L. Avanov, A. Barrie, V. Coffey, J. Dorelli, D. Gershman, B. Giles, T. Rosnack, C. Salo, S. Yokota, M. Adrian, C. Aoustin, C. Auletti, S. Aung, V. Bigio, N. Cao, M. Chandler, D. Chornay, K. Christian, G. Clark, G. Collinson, T. Corris, A. De Los Santos, R. Devlin, T. Diaz, T. Dickerson, C. Dickson, A. Diekmann, F. Diggs, C. Duncan, A. Figueroa-Vinas, C. Firman, M. Freeman, N. Galassi, K. Garcia, G. Goodhart, D. Guererro, J. Hageman, J. Hanley, E. Hemminger, M. Holland, M. Hutchins, T. James, W. Jones, S. Kreisler, J. Kujawski, V. Lavu, J. Lobell, E. LeCompte, A. Lukemire, E. MacDonald, A. Mariano, T. Mukai, K. Narayanan, Q. Nguyan, M. Onizuka, W. Paterson, S. Persyn, B. Piepgrass, F. Cheney, A. Rager, T. Raghuram, A. Ramil, L. Reichenthal, H. Rodriguez, J. Rouzaud, A. Rucker, Y. Saito, M. Samara, J.-A. Sauvaud, D. Schuster, M. Shappirio, K. Shelton, D. Sher, D. Smith, K. Smith, S. Smith, D. Steinfeld, R. Szymkiewicz, K. Tanimoto, J. Taylor, C. Tucker, K. Tull, A. Uhl, J. Vloet, P. Walpole, S. Weidner, D. White, G. Winkert, P.-S. Yeh, and M. Zeuch. Fast plasma investigation for magnetospheric multiscale. *Space Sci. Rev.*, 199(1):331–406, Mar 2016.

16. B. Rossi and S. Olbert. *Introduction to the Physics of Space*. New York: McGraw-Hill, 1970.
17. L. Spitzer. *Physics of Fully Ionized Gases*. New York: Interscience Publishers, 1956.
18. M. Strumik, A. Czechowski, S. Grzedzielski, W. M. Macek, and R. Ratkiewicz. Small-scale local phenomena related to the magnetic reconnection and turbulence in the proximity of the heliopause. *Astrophys. J. Lett.*, 773:L23, 2013.
19. M. Strumik, S. Grzedzielski, A. Czechowski, W. M. Macek, and R. Ratkiewicz. Advective transport of interstellar plasma into the heliosphere across the reconnecting heliopause. *Astrophys. J. Lett.*, 782:L7, 2014.
20. R. B. Torbert, J. L. Burch, B. L. Giles, D. Gershman, C. J. Pollock, J. Dorelli, L. Avanov, M. R. Argall, J. Shuster, R. J. Strangeway, C. T. Russell, R. E. Ergun, F. D. Wilder, K. Goodrich, H. A. Faith, C. J. Farrugia, P.-A. Lindqvist, T. Phan, Y. Khotyaintsev, T. E. Moore, G. Marklund, W. Daughton, W. Magnes, C. A. Kletzing, and S. Bounds. Estimates of terms in Ohm's law during an encounter with an electron diffusion region. *Geophys. Res. Lett.*, 43:5918–5925, June 2016.
21. R. B. Torbert, J. L. Burch, T. D. Phan, M. Hesse, M. R. Argall, J. Shuster, R. E. Ergun, L. Alm, R. Nakamura, K. J. Genestreti, D. J. Gershman, W. R. Paterson, D. L. Turner, I. Cohen, B. L. Giles, C. J. Pollock, S. Wang, L.-J. Chen, J. E. Stawarz, J. P. Eastwood, K. J. Hwang, C. Farrugia, I. Dors, H. Vaith, C. Mouikis, A. Ardakani, B. H. Mauk, S. A. Fuselier, C. T. Russell, R. J. Strangeway, T. E. Moore, J. F. Drake, M. A. Shay, Y. V. Khotyaintsev, P.-A. Lindqvist, W. Baumjohann, F. D. Wilder, N. Ahmadi, J. C. Dorelli, L. A. Avanov, M. Oka, D. N. Baker, J. F. Fennell, J. B. Blake, A. N. Jaynes, O. Le Contel, S. M. Petrinec, B. Lavraud, and Y. Saito. Electron-scale dynamics of the diffusion region during symmetric magnetic reconnection in space. *Science*, 362:1391–1395, December 2018.
22. R. A. Treumann. Fundamentals of collisionless shocks for astrophysical application, 1. Non-relativistic shocks. *Astronom. Astrophys. Rev.*, 17:409–535, 2009.
23. R. A. Treumann and W. Baumjohann. Collisionless magnetic reconnection in space plasmas. *Frontiers in Physics*, 1:31, 2013.
24. V. M. Vasyliunas. Theoretical models of magnetic field line merging. I. *Rev. Geophys. Space Phys.*, 13:303–336, 1975.
25. R. Wang, Q. Lu, R. Nakamura, W. Baumjohann, C. Huang, C. T. Russell, J. L. Burch, C. J. Pollock, D. Gershman, R. E. Ergun, S. Wang, P. A. Lindqvist, and B. Giles. An Electron-Scale Current Sheet Without Bursty Reconnection Signatures Observed in the Near-Earth Tail. *G. Res. Lett.*, 45:4542–4549, May 2018.
26. J. M. Webster, J. L. Burch, P. H. Reiff, A. G. Daou, K. J. Genestreti, D. B. Graham, R. B. Torbert, R. E. Ergun, S. Y. Sazykin, A. Marshall, R. C. Allen, L.-J. Chen, S. Wang, T. D. Phan, B. L. Giles, T. E. Moore, S. A. Fuselier, G. Cozzani, C. T. Russell, S. Eriksson, A. C. Rager, J. M. Broll, K. Goodrich, and F. Wilder. Magnetospheric Multiscale Dayside Reconnection Electron Diffusion Region Events. *J. Geophys. Res.*, 123:4858–4878, June 2018.
27. E. Yordanova, Z. Vörös, A. Varsani, D. B. Graham, C. Norgren, Y. V. Khotyaintsev, A. Vaivads, E. Eriksson, R. Nakamura, P.-A. Lindqvist, G. Marklund, R. E. Ergun, W. Magnes, W. Baumjohann, D. Fischer, F. Plaschke, Y. Narita, C. T. Russell, R. J. Strangeway, O. Le Contel, C. Pollock, R. B. Torbert, B. J. Giles, J. L. Burch, L. A. Avanov, J. C. Dorelli, D. J. Gershman, W. R. Paterson, B. Lavraud, and Y. Saito. Electron scale structures and magnetic reconnection signatures in the turbulent magnetosheath. *Geophys. Res. Lett.*, 43:5969–5978, June 2016.